On the route to shear jamming, are fragile states real?

Ling Zhang[1], Jie Zheng[1] and Jie Zhang[1,2] [(a)]

[1] *Department of Physics and Astronomy, Shanghai Jiao Tong University - Shanghai 200240, China*
[2] *Institute of Natural Sciences, Shanghai Jiao Tong University - Shanghai 200240, China*

PACS 83.80.Fg – Granular solids (rheology)
PACS 45.70.-n – Granular systems
PACS 81.05.Rm – Porous materials; granular materials

Abstract – Starting from an unjammed initial state, applying shear to a granular material of a fixed packing fraction below ϕ_J, i.e. the isotropic jamming density of frictionless spheres can produce shear jamming states, as have been discovered recently. In addition, it has also been discovered that the system will first experience a bulk fragile state before evolving into a shear jammed state. Due to the existence of friction between the system and the third dimension in the previous studies, it is unclear whether such fragile state would still exist on the route to shear jamming if the friction with the third dimension were completely eliminated and the background noise level were greatly reduced. Using a novel apparatus, we have completely eliminated the friction between particles and the third dimension by floating the particles on the surface of a shallow water layer thus revealing more details of the route of shear-jamming. We are able to measure weak boundary pressure of three orders of magnitude below the resolution of the photo-elastic method through the combination force-gauges of high sensitivity and a cantilever-like simple-beam apparatus. In a system with weak cohesion, we have indeed observed the bulk fragile states before the shear jamming; in addition, we have also discovered the boundary fragile states and regimes of negligible shear modus compared to bulk modulus. Most importantly, we now have a much better understanding of the bulk fragile state: its existence requires an auxiliary in some form, e.g. the weak cohesion in this experiment. By constructing a way to freely tune down the cohesion to more than six orders of magnitude smaller, to our surprise, we have discovered the complete vanishing of the bulk fragile states, which thus allows us to determine the plausible origin of the bulk fragile state.

Introduction. – Dry granular material with a purely repulsive interaction between grains can show a fascinating transition from a liquid-like to a solid-like state [1, 2] with classical examples such as the sudden arrest of flow in a hopper in an industry application to more general examples such as the traffic jam on a highway and the intermittent flow of living animals rushing through a gate [3]. Understanding such a phenomenon is, however, a great challenge since a granular material is athermal and out of equilibrium. The jamming-phase diagram provides an intuitive picture on how frictionless particles in an isotropic system can become jammed upon the increase of the packing fraction [4], where a critical-like transition has been discovered for frictionless spherical particles near the J-point in the numerical simulation [5] and has been observed in the studies of foams [6], emulsions [7], photoelastic disks [8], and colloids [9]. More details can be found in the recent review articles [10, 11]. Compared with the isotropic jamming, the recently discovered shear jamming is less intuitive in the way a system can gain rigidity under the application of the shear strain to the system of a fixed packing fraction [12–17]. Phenomenological theoretical models have been proposed to analyse the process in force space in order to understand the origin of rigidity [18, 19] or to adopt a Landau-type theory for non-equilibrium first order phase transition [20]. Recently, shear jamming in frictionless particle systems has been discovered in numerical simulations [21, 22].

The existing experiments have explored the shear jamming process in 2D system in order to eliminate the gravity, where photoelastic disks have been used to detect the evolution of force-chain networks in shearing processes [12, 13, 15–17]. The shear-jammed states are robust under

[(a)] Email: jiezhang2012@sjtu.edu.cn

different experimental protocols, which include the driving from the boundary with [12, 13, 15] and without [17] the bottom friction and the driving through the homogeneous shear [16]. However, concerns remain regarding the transition from an unjammed state to a shear-jammed state, in particular, the bulk fragile state discovered in [15] through analysing the percolation of the force-chain network. Here the main issue is that the detection of the force network using photoelastic disks has a pressure resolution limit on the order of $\sim 1N/m$, causing difficulties in studying the dynamics in the vicinity of the shear-jamming transition. This has motivated the present work to improve the force resolution to resolve carefully the dynamics near the shear-jamming transition.

In this study, we have successfully designed a new experimental setup to achieve a pressure resolution down to $3 \times 10^{-4} N/m$, which is more than three orders of magnitude smaller compared to the previous photoelastic method. This provides us with the privilege to analyse the transition regime in the shear-jamming process with much greater details for the first time in an experiment. Here we show that in a system of weak cohesion the bulk fragile state can indeed be observed before the system evolves into a shear-jammed state, where in the biax under pure shear the rise of the pressure precedes on the compressional boundaries than on the dilatational boundaries. In addition, for such a system at lower packing fractions, we also occasionally observe a novel fragile state which is consistent with the boundary fragile state proposed by Cates and colleagues [2]. Moreover, we have also observed that the system can enter into a marginal state with a negligible shear modulus compared with the bulk modulus before the system further evolves to the stable shear jammed state, which resembles the mechanical response of the isostatic state [10,11]. By constructing a new mushroom-type particles, we can greatly tune down the cohesion of the system to more than six orders of magnitude. In such a system of negligible cohesion, we have observed no bulk fragile states, where the pressure on both the compression and dilation directions grows simultaneously.

Experimental methods. – The experiments are carried out using a biax similar to the ones in Ref. [12, 13, 15], where pure shear can be applied to gradually deform a square frame into a rectangular shape while keeping the area and thus the packing fraction fixed. However, there are two major differences here: first, in the present setup the boundary motion is more symmetric, i.e. four walls are mobil while the center of mass of the system is fixed; second, the system is filled with a shallow layer of water with particles floating on the surface of the water to remove the friction between the particles and the horizontal bottom plate, similar to Ref. [17] where particles are immersed in the density matched fluid instead. The schematic diagram of the biax can be seen in Fig. 1, where the pure shear is the symmetric compression of one pair of walls (sketched using two red arrows) with the simultaneous expansion of another pair of walls (the two blue arrows) under the fixed area of the system.

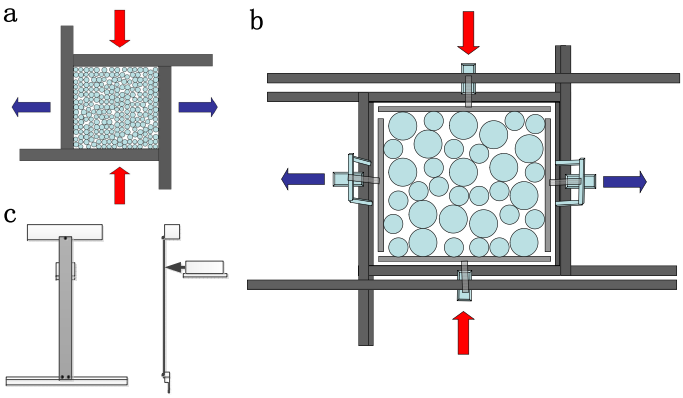

Fig. 1: The schematic diagram of the experimental apparatus. (a) The schematic of the square cell filled with ∼1900 bi-disperse photo-elastic disks, where each disk is floating on a shallow water layer to eliminate the friction between the disks and the horizontal bottom plate. The initial size of the square cell is $56.3cm \times 56.3cm$, where pure shear can be applied to deform the cell into rectangular shape by keeping the cell area fixed. (b) To increase the accuracy of the force measurement substantially, the same setup can be used to apply pure shear to about 40 bi-disperse plastic disks floating on the water surface. For such a small system, small boundary forces can be measured through a combination of T-shaped cantilever and force gauges of high precision of 0.001 N. The four force gauges are mounted on top of the four boundary walls. (c)A close-up front and side views of the force-measurement device, which consists of an inverse T-shaped cantilever made of a 50 cm long ruler connected with a vertical bar of 30 cm long in the center. The horizontal ruler of the cantilever is in direct contact with the disks and top of the cantilever is mounted at a fixed position. The tip of the force-gauge is in marginal contact with the vertical stainless steel ruler a few center meters below the mounted fixed position to achieve an amplification factor ∼8.0.

Using this apparatus, we first applied pure shear to $\sim$ 1900 bi-disperse photoelastic disks (large disk of size 1.4 cm and small disk of size 1.0 cm) at a fixed packing fraction of $\phi = 0.809 \pm 0.002$ and we found the qualitatively similar results compared to the previous studies [12,13,15]. Figure 2 shows a portion of the force-chain network at four different linear strains. In the beginning, the system is unjammed as shown in Fig. 2(a) and at a sufficiently large strain the system are clearly in shear-jammed states as shown in Fig. 2(c-d). In between, Fig. 2(b) is suggestive that the system might go through a fragile state where force-chains seem to develop first along the compression direction. However, it is still an unresolved problem whether such a fragile state truly exists due to the limitation of the force resolution.

Because the typical pressure resolution limit is on the order of $\sim 1N/m$ in 2D, it is not reliable to detect the stress evolution through the analysis of the force chains network in order to examine the behavior of the system

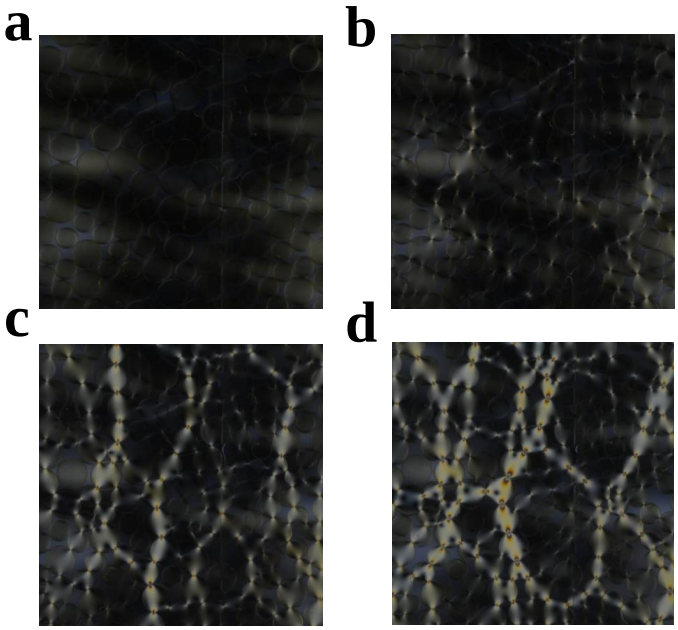

Fig. 2: The development of the force chain networks during one typical shear-jamming process. To provide a close view, the four images are selected from the center of the whole system, covering $\frac{1}{16}$ of the area fraction when the packing fraction of the whole system is fixed at 0.809 ± 0.002. In the beginning the system is unjammed with zero stress as shown in image (a) and as shear is applied, shear jammed states can be developed as shown in panels (c-d). Panel (b) is suggestive that a bulk fragile state might be developed during the shear jamming process.

close to the shear jamming transition. It is thus a great challenge to directly detect the particle-scale contact force below the photoelastic limit. Hence we directly measure the boundary force instead. To achieve a better resolution of weak forces, we use force gauges of a precision of $0.001N$ in order to measure the boundary force. Further more, we have designed a cantilever-like mechanical device to amplify the boundary force by a factor of ~ 8 compared to the force directly measure from a force gauge.

A schematic diagram of the force measurement can be seen in Fig. 1(b-c). Here panel (b) shows the top view of the device, where each force gauge is installed on a linear translation stage mounted on top of the respective wall bank made of Aluminum bar. Panel (c) shows the front view (left) and the side view (right) of the cantilever-like mechanical device consisting the inverse 'T'-shape-like structure made of a rigid horizontal bar and a stainless steel ruler. One end of the ruler is fixed at the top of the boundary and the other end is connected to the middle of the horizontal rigid bar. The four bars are inserted into the original rectangular frame of the biax, forming a smaller rectangular regime. The flat tip of the force gauge is adjusted to barely touch the upper part of the ruler at the start of a given experimental run. With such a design, we can achieve a boundary pressure resolution of $3 \times 10^{-4} N/m$, which is at least three orders of magnitude

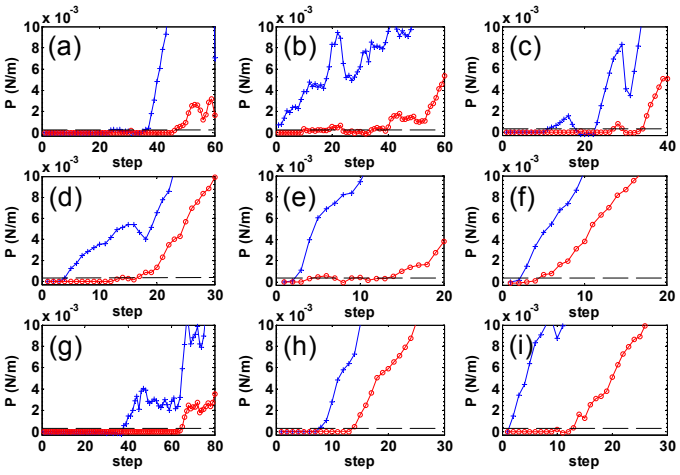

Fig. 3: The boundary pressure along the compression (blue +) and expansion (red ∘) directions versus linear strain of the compression direction. Here each step is equivalent to an increment of the linear strain of $\delta\epsilon = 3.55 \times 10^{-4}$. Each panel shows results from one experimental run and the packing fraction $\Phi = 0.775 \pm 0.002$. The dashed lines indicate the uncertainty of the pressure measurement of $3 \times 10^{-4} N/m$. Here all runs show consistent bulk fragile state before the shear jammed state.

smaller compared with the photoelastic method.

After a substantial gain of the pressure resolution, we have to reduce the number of particles down to ~ 40 larger bi-disperse plastic disks floating on the water surface as shown in Fig. 1(b). The reasons are the following. If smaller-size ($\sim 1cm$) photoelastic disks were used, disks would flow through the corners between the four bars causing stuck of the disks between the bar and the wall; on the other hand, if the gap at the corner between the bars were reduced, the maximum strain of the shear would be reduced substantially. For these reasons, we have to compromise the system size though we believe the results shall be qualitatively the same even with a much bigger system size.

All mutually contacted areas between the plastic disks and the four bars have been coated with Teflon tapes to substantially minimize the tangential component of the forces applied by the four boundaries. In this study, we have performed pure shear at three different packing fractions, and at each packing fraction we have repeated the experiment for multiple times. Each time, the system is quasi-statically pure- sheared up to a few hundred steps, with each step equivalent to a linear strain increment of 3.55×10^{-4}. After each experimental run, the initial configurations of the disks has been rearranged following the same protocol to create a new random configuration.

Results and Discussions. – Figure 3 shows a set of results of the evolution of the boundary pressure as a function of linear strain along the compression (blue +) and the expansion (red ∘) directions at the packing fraction $\Phi = 0.775 \pm 0.002$. In this figure, the linear strain on the

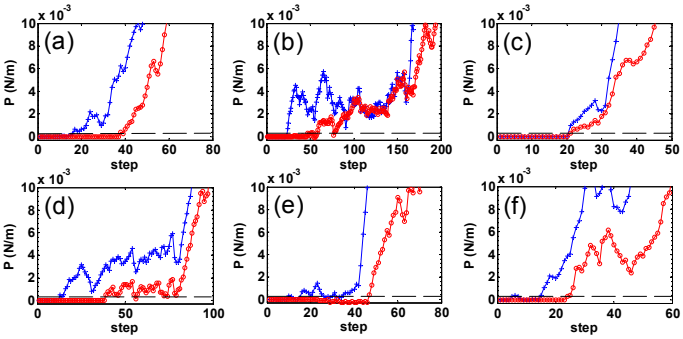

Fig. 4: The boundary pressure along the compression (blue +) and expansion (red ○) directions versus linear strain of the compression direction, similar with Fig. 3 at $\Phi = 0.766 \pm 0.002$.

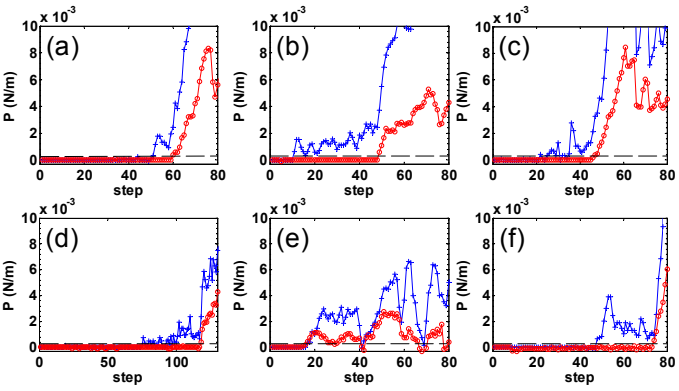

Fig. 5: The boundary pressure along the compression (blue +) and expansion (red ○) directions versus linear strain of the compression direction, similar with Fig. 3 at $\Phi = 0.757 \pm 0.002$.

horizontal axis is plotted using the step instead, which can be directly converted to the linear strain by multiplying the constant $\delta\epsilon = 3.55 \times 10^{-4}$. Here each panel of Fig. 3 represents an independent experimental run at the same Φ. All panels show that the pressure along the compression direction grows first while the pressure along the expansion direction remains zero for a finite regime of strain before it starts to grow. Here the resolution of the measurement of the boundary pressure is $3 \times 10^{-4} N/m$, as estimated from the resolution of the force gauge and some relevant constants related to the mechanical structure of the cantilever and the length of the rigid bar at the boundary. This pressure resolution is drawn using the dashed line in each panel of Fig. 3, where any pressure below this limit is zero.

The bulk fragile state proposed by Cates et. al. describes straight force-chains that can only support compression forces along the force-chain direction while the supporting forces at the perpendicular direction are zero [2]. Hence if the bulk fragile state does exist near the shear-jamming transition, the ratio $\xi \equiv \frac{p_c}{p_e}$ will be infinitely large since p_e is infinitesimally small and p_c is finite, where p_c is the pressure of the compression direction and p_e is the pressure of the expansion direction. In a real experiment, however, no infinitesimal p_e can be measured since all measurements have uncertainties. Based on the uncertainty of the pressure measurement, we can estimate the lower bound of ξ near the shear jamming transition. Here we choose $p_e = 3 \times 10^{-4} N/m$, i.e. the pressure resolution as a maximal estimation of p_e. In panels (a-c,e, i) of Fig. 3, $p_c \approx 10 \times 10^{-3} N/m$, which yields a ratio of $\xi \geq 33$. Similarly, other panels of Fig. 3 yield a ratio of $\xi \geq 10$. In our experiment, we consider the existence of a bulk fragile state if $\xi \geq 10$. Therefore, Fig. 3 shows a consistent picture of the bulk fragile state [2].

Figure 4 shows another set of results at a lower packing fraction $\Phi = 0.766 \pm 0.002$. Here, the results are more complex. $\xi \geq 10$ in panels(a,e,f) of Fig. 4, showing the existence of bulk fragile states similar to Fig. 3. However, results in other panels are less clear. In Fig. 4(b), when the two pressure curves both grow above zero around the step 50, $\xi \geq 6$, so it is less certain of the existence of the bulk fragile states before the system is shear jammed. Around the step 75, p_e suddenly drops to zero before it rises above zero again. The state near the step 75 resembles the boundary fragile state proposed in Cates et. al.'s paper [2], where an incompatible load at the boundaries will cause the system to unjam. In Fig. 4(b), there is also a considerable range of strain, about 100 steps, showing that the two pressure curves are very close to each and thus suggesting that the shear modulus is considerably smaller than the bulk modulus of the system. Remarkably, such a behavior resembles the features of the soft modes of frictionless systems near the jamming transition [10,11] though cautions must be taken that here the system must be anisotropic instead. In Fig. 4(c), two pressure curves grow nearly simultaneously above zero, indicating the absence of the bulk fragile state when the unjammed states start to make transition to the shear jammed states. In Fig. 4(d), the system also shows the existence of boundary fragile states before it eventually enters into a stable shear jammed regime.

In Fig. 5, ϕ is further reduced to $\phi = 0.757 \pm 0.002$, where in panels (a-d,f) the values of $\xi < 10$ near the shear jamming transition, which makes it less certain to distinguish the actual bulk fragile states. Fig. 5(e) shows that p_c and p_e increase simultaneously and within a finite regime of strain the shear modulus remains much smaller compared to the bulk modulus; the system remains shear jammed for a finite strain and then the boundary fragility appears. Such behavior is then repeated a few times, resembling the behavior seen in Figs. 4(b-d).

One important issue is regarding to the role of the surface tension. It is well known that when small objects floating on the surface of water the surface curvature will be distorted and may create an effective attraction between particles, i.e. the cheerio's effect [23, 24]. In our system, we do observe the weak attraction between a pair of particles though the force magnitude is rather small. We have estimated that such a cohesion force will cause

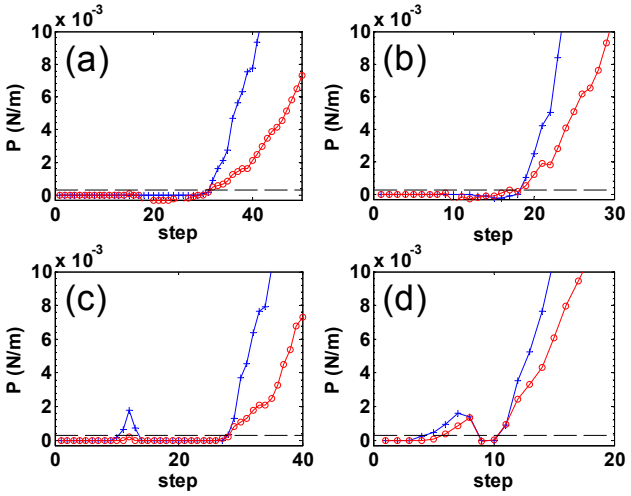

Fig. 6: The boundary pressure along the compression (blue +) and expansion (red ○) directions versus linear strain of the compression direction, similar with Fig. 3 except that here the cohesion force between disks has been greatly reduced, e.g. at least 6 orders of magnitude smaller between a pair of small disks and 14 orders magnitude between a pair of small and large disks. In panels (a-b), $\Phi = 0.785 \pm 0.002$ and in panels (c-d), $\Phi = 0.774 \pm 0.002$.

an effective stress at least an order of magnitude smaller than the present pressure resolution. We have performed a related experiment to access the possible connection between the weak cohesion and the fragile states discussed above.

In the new experiment, we have carefully designed a new mushroom-like particle by gluing a larger plastic disk on top of a smaller plastic disk with disk centers aligned. In such a way, when one mushroom-like particle is floating on the water surface, only the particle's bottom disk is in direct contact with water. Hence two mushroom particles are in direct contact through the contact of the two top disks, causing an effective separation distance between the meniscus of two bottom disks to be at least $14mm$, e.g. if two small mushroom-like particles are in contact. As a consequence, the cohesion between two mushroom-like particles can be tuned down at least one million times smaller compared with the cohesion force between particles used to obtain results in Figs. (3-5). This is because the cohesion force decays exponentially as the ratio of the separation distance over the capillary length increases. The results are remarkable: the bulk fragile state disappears and instead we have observed that the pressure of the compression and expansion directions grows simultaneously from above zero at the shear jamming transition within the uncertainty, as seen in Fig. 6. The boundary fragile state can still be observed in Fig. 6(d), and possibly also in the small bump of Fig 6(c).

Further discussions and conclusion. – Before we conclude the paper, there are a few remarks we want to make. The first remark is regarding the finite size of the system. The total number of particles in the present system is small due to the experimental difficulties discussed early in the paper. We believe the increase of the particle numbers will only make a quantitative but not a qualitative difference, as is suggested by the simulation done by Ning Xu's group [25]. Our present experiment should be viewed more as a demonstration of principle. The bulk fragile states observed in the high packing fraction case also seem to be consistent with the observation from the photoelastic experiment where much more particles are used though the later is not able to directly measure the vicinity of the shear jamming transition regime but may still provide a meaningful comparison.

The second remark is regarding the friction between particles. The particles have been wrapped with the teflon tape to reduce the friction coefficient to 0.1, which is the minimum value we can achieve so far; increasing the friction coefficient, however, does not make a qualitative difference. Recent simulations by Luding's group and Ohern's group have independently demonstrated the existence of shear jamming for frictionless particles [21, 22], though we still have not completely understood the direct implication of their discoveries to the present experiment. The findings in Fig. 4(b) and Fig. 5(e) are rather remarkable, which show the negligible ratio between the shear modulus and the bulk modulus. Is this behavior resembling the frictionless particles in shear jamming? We do not know yet.

In conclusion, we have measured the stress evolution near the shear jamming transition in a quasi-2D system. By combining a cantilever-like mechanical device and force gauges of high sensitivity, we have achieved a remarkable weak stress measurement of an uncertainty $3 \times 10^{-4} N/m$, which is at least three orders of magnitude below the typical photo-elastic measurement. At a sufficiently large packing fraction, the bulk fragile state is first encountered before the system is shear jammed. This behavior is consistent with the early findings in the photoelastic measurements [12, 13, 15–17]. At smaller packing fractions, though in a majority of runs, pressure of the compression direction rises above zero while pressure of the expansion direction remains zero, it is less conclusive to distinguish such bulk fragile states from the state where pressure rises simultaneously along both directions. Interestingly, we have discovered the boundary fragile state before the system evolves into the shear jammed state, which has not been reported in experiments in the literature, to our best knowledge. Moreover, we have discovered a novel state where the shear modulus is much smaller than the bulk modulus near the shear jamming transition, which might be relevant to the shear jamming in frictionless particle systems [21, 22]. Finally, we have now had a much better understanding of the origin of the bulk fragile states. In order to observe the bulk fragile states before shear jamming, an auxiliary must exist. Now this produces a coherent physical picture for the bulk fragile state reported in various experiments, e.g. in the existence of the friction

between photoelastic particles and the horizontal bottom surface [12, 15, 16] and the weak cohesion in this experiment. Hence we believe that the bulk fragile state may also be observable in systems of very large friction between particles and in systems of strong particle entanglement, e.g. [26]. Without such an auxiliary, i.e. force/physical property, a given system will make a direct transition from an unjammed state to a shear jammed state, with possibly the boundary fragile state in between.

* * *

J.Z. acknowledges support from the award of the Chinese 1000-Plan (C) fellowship, Shanghai Pujiang Program (13PJ1405300), and National Natural Science Foundation of China (11474196).

REFERENCES

[1] Jaeger Heinrich M., Nagel Sidney R. and Behringer Robert P., *Rev. Mod. Phys.*, **68** (1996) 1259.
[2] Cates M.E., Wittmer J.P., Bouchaud J.-P. and Claudin P.h., *Phys. Rev. Lett.*, **8** (1998) 1841.
[3] Garcimartín A., Pastor J.M., Ferrer L.M., Ramos J.J., Martín-Gómez C. and Zuriguel I., *Phys. Rev. E*, **91** (2015) 022808.
[4] Liu Andrea J. and Nagel Sidney R., *Nature*, **396** (1998) 21.
[5] OHern Corey S., Silbert Leonardo E., Liu Andrea J. and Nagel Sidney R., *Phys. Rev. E*, **68** (2003) 011306.
[6] Durian D.J., *Phys. Rev. Lett.*, **75** (1995) 4780.
[7] Brujić Jasna, Edwards Sam F., Hopkinson Ian, and Makse Hernán A., *Physica A: Statistical Mechanics and its Applications*, **327** (2003) 201.
[8] Majmudar T.S., Sperl M., Luding S. and Behringer Robert P., *Phys. Rev. Lett.*, **98** (2007) 058001.
[9] Zhang Zexin, Xu Ning, Chen Daniel T.N., Yunker Peter, Alsayed Ahmed M., Aptowicz Kevin B., Habdas Piotr, Liu Andrea J., Nagel Sidney R. and Yodh Arjun G., *Nature*, **459** (2009) 230.
[10] Liu Andrea J. and Nagel Sidney R., *Annu. Rev. Condens. Matter Phys.*, **1** (2010) 347.
[11] Van Hecke M., *J. Phys.: Condens. Matter*, **22** (2010) 033101.
[12] Zhang J., Majmudar T.S., Tordesillas A., and Behringer R.P., *Granular Matter*, **12** (2010) 159.
[13] Zhang J., Majmudar T.S., Sperl M., and Behringer R.P., *Soft Matter*, **6** (2010) 2982.
[14] Otsuki Michio and Hayakawa Hisao, *Phys. Rev. E*, **83** (2011) 051301.
[15] Bi Dapeng, Zhang Jie, Chakraborty Bulbul, and Behringer R.P., *Nature*, **480** (2011) 355.
[16] Ren Jie, Dijksman Joshua A., and Behringer R.P., *Phys. Rev. Lett.*, **110** (2013) 018302.
[17] Zheng Hu, Dijksman Joshua A., and Behringer R.P., *EPL (Europhys. Lett.)*, **107** (2014) 34005.
[18] Sarkar Sumantra, Bi Dapeng, Zhang Jie, Behringer R.P. and Chakraborty Bulbul, *Phys. Rev. Lett.*, **111** (2013) 068301.
[19] Sarkar Sumantra and Chakraborty Bulbul, *Phys. Rev. E*, **91** (2015) 042201.
[20] Grob Matthias, Heussinger Claus and Zippelius Annette, *Phys. Rev. E*, **89** (2014) 050201.
[21] Kumar Nishant and Luding Stefan, *arXiv preprint arXiv:1407.6167*, **1407** (2014) 6167.
[22] Bertrand Thibault, O'Hern Corey S., Behringer R.P., Chakraborty Bulbul and Shattuck Mark D., *APS March Meeting 2015*, **60** (2015) 1.
[23] Vella Dominic and Mahadevan L., *American J. Phys.*, **73** (2005) 817.
[24] Cooray Himantha, Cicuta Pietro and Vella Dominic, *J. Phys.: Condens. Matter*, **24** (2012) 284104.
[25] Zheng Wen, Liu Hao and Xu Ning, *Private Communications*, (2014) .
[26] Gravish Nick, Franklin Scott V., Hu David L., and Goldman Daniel I., *Phys. Rev. Lett.*, **108** (2012) 208001.